J. exp. Biol. **144**, 81–111 (1989)
Printed in Great Britain © *The Company of Biologists Limited 1989*

PROCESSING OF SENSORY INPUT FROM THE FEMORAL CHORDOTONAL ORGAN BY SPIKING INTERNEURONES OF STICK INSECTS

BY ANSGAR BÜSCHGES

Fachbereich Biologie, Universität Kaiserslautern, 6750 Kaiserslautern, Federal Republic of Germany

Accepted 3 April 1989

Summary

The femoral chordotonal organ (ChO) of the right middle leg of the inactive stick insect *Carausius morosus* was stimulated by applying movements having a ramp-like time course, while recordings were made from local and interganglionic interneurones in the anterior ventral median part of the ganglion. Position, velocity and acceleration of the movements were varied independently and the interneurones were categorized on the basis of their responses to the changes in these parameters. Position-sensitivity was always accompanied by responses to velocity and/or acceleration. Velocity-sensitive responses were excitatory or inhibitory and were produced by elongation or relaxation, or by both. In some cases, velocity-sensitive neurones were also affected by position and acceleration. Acceleration responses were always excitatory and were often found in neurones that showed no effects of velocity or position. It is inferred that sensory input from different receptors in the ChO is processed by single interneurones. No interneurone in the recording region was found to be directly involved in the resistance reflex of the extensor tibiae motoneurones, elicited by stimulation of the ChO.

Introduction

A walking animal requires continuous input from different proprioceptive sense organs measuring position and movement of its appendages. Invertebrates have often been used for the study of walking and other behaviour because they offer the advantages of a simple nervous system and simple types of behaviour (Bässler, 1983). Studies of walking in stick insects have advanced our understanding of the coordination of legs, as well as the control of single joints of legs, during walking. The inputs and outputs of feedback loops controlling the position and movement of different joints, particularly the femur–tibia joint, have been investigated in great detail (for reviews see Bässler, 1983, 1988).

The input to the feedback loop that controls the femur–tibia joint has been investigated by studying the main proprioceptive sense organ of this joint, the femoral chordotonal organ (ChO). This organ contains receptor units sensitive to

Key words: stick insect, spiking interneurones, central processing, chordotonal organ.

position, velocity and acceleration of the tibia, as well as units that respond to various combinations of these parameters (Hofmann *et al.* 1985; Hofmann & Koch, 1985). The motor output of this joint-controlling system can show one of two different responses during stimulation of the ChO, depending on the behavioural state of the animal (Bässler, 1976, 1983, 1988). In the inactive animal the motor output to the extensor and flexor muscles is that of a resistance reflex, which means that the joint-controlling muscles 'try' to resist the imposed movement. In the active animal the resistance reflex is not detectable. Instead, stimuli signalling flexion movements elicit activity in the flexor muscle, and that means a positive feedback, called the 'active reaction' (reflex reversal; for details see Bässler, 1988). These two kinds of motor output have been shown to be produced by separate neural channels (Bässler, 1988).

Although the input and output of the joint-controlling system of the femur–tibia joint are well understood, nothing is known about the processing of the sensory input and the central circuits mediating the different types of behaviour. This is also true for all other feedback loops that control leg movements in phasmids (Schmitz, 1986*a*,*b*).

In locusts, the central connectivity between the input and output is at least partly known (Burrows, 1987; Laurent, 1986, 1987*a*,*b*). Sensory cells of the ChO have been shown to convey parallel information to interneurones and motoneurones (Burrows, 1987). However, in locusts, the detailed physiology of the femoral ChO, the systems analysis of the feedback loops, and the dependence of the function of these loops upon the behavioural context, are all unknown. However, the investigations on locusts have shown groups of interneurones that are involved in the processing of sensory input from the legs (e.g. the midline group of spiking local interneurones, Burrows, 1985; intersegmental interneurones, Laurent, 1986, 1987*a*,*b*, 1988). Burrows (1988) has shown that position and velocity signals from the ChO are processed by some spiking local interneurones of the midline group.

The present paper describes the physiology and morphology of interneurones representing the sensory input of the ChO in the anterior ventral median part of the mesothoracic ganglion of *Carausius morosus* in the inactive state. This investigation supplies data which help to bridge the gap between the quantitative analyses of the input and output systems in the stick insect. It combines methods of systems analysis with the technique of intracellular recording from spiking interneurones.

The main emphasis is on the question of how position, velocity and acceleration are processed in a certain part of the ganglion in the inactive animal. In addition a characterization of certain interneurones is also achieved.

Materials and methods

All experiments were performed on adult female *Carausius morosus* from our colony at the University of Kaiserslautern. The animals were mounted ventral-side up on a platform (Fig. 1). The middle legs and the meso- and metathoracic

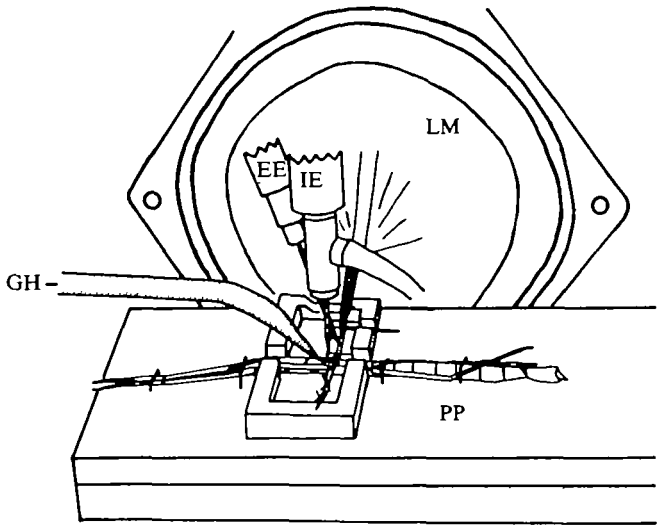

Fig. 1. Schematic drawing of the experimental set-up. The animal was placed ventral-side up on the platform. LM, loudspeaker membrane carrying the paper cone with the stimulation clamp; EE, extracellular hook electrode; IE, intracellular electrode holder; GH, ganglion holder; PP, preparation platform.

segments were placed inside an enclosure (20 mm × 60 mm) which was filled with *Carausius* saline (Weidler & Diecke, 1969). The left middle leg was fixed perpendicular to the thorax, and turned so that the anterior side of the femur was facing up. The tibia was positioned perpendicular to the femur. A small opening was made in the anterior distal part of the femur and the receptor apodeme of the femoral chordotonal organ (ChO) was fixed in a small clamp and cut distal to the clamp. The apodeme clamp could be moved in a controlled way to generate stimulation of the ChO. Trapezoidal displacements of 100 μm amplitude from the right-angle position were applied to the ChO, most often in the elongation (= positive) direction, in some cases in the relaxation (= negative) direction as well. (During leg flexion the ChO is elongated.) Changing the length of the receptor apodeme by 100 μm corresponds to a change of about 20° in the angle between femur and tibia in *Carausius* (Weiland *et al.* 1986). Thus, the range of stimuli applied to the ChO corresponded to a joint angle ranging between approximately 70° and 90° (exceptionally between 70° and 110°).

In this paper the stimulus characteristics are mainly given in the units appropriate to describe the direct elongation and relaxation of the ChO – mm, $mm\,s^{-1}$ ($m\,s^{-1}$) and $mm\,s^{-2}$ ($m\,s^{-2}$). One could argue that describing the corresponding tibia movement, i.e. 'flexion' and 'extension', measured in degrees of the femur–tibia angle, would yield a more appropriate and natural description of the situation. However, there are several reasons against this. (1) The receptor apodeme of the ChO is attached to the tibia in such a way that the transduction of the angular change is not linear (Weiland *et al.* 1986). Therefore, the use of angular

units is not exact. (2) There are principally two ways to stimulate the ChO. One is to bend the whole tibia, either by active movements or by imposed forces. The other is to move the receptor apodeme without moving anything else. In the first type of experiment (where angular units are appropriate), the studied interneurones could receive input from many different sense organs in addition to the ChO. Thus, direct stimulation of the ChO is the only adequate method. The use of angular units in our situation would suggest an equivalence of the two experimental situations, which is certainly not the case. Nevertheless, as an aid to understanding, angular units describing the mimicked movements of the femur–tibia joint (degrees s^{-1}, degrees s^{-2}) are appended in brackets. In the same way flexion and extension are sometimes used to explain the stimulus to the ChO.

For intracellular recordings the body was opened from the ventral side. Connective and fat tissue were removed and the mesothoracic ganglion was lifted onto a wax-coated platform and fixed with small cactus needles. The ganglion sheath was treated for 1 min with Pronase (Sigma type XIV). Recording and staining were made using glass microelectrodes, filled with 4% Lucifer Yellow (Stewart, 1978) and 1 mol l^{-1} LiCl, having a resistance of 50–90 MΩ. The interneurones were stained by passing continuous negative current (−5 to −15 nA) for about 15 min. The ganglion was then removed and fixed for 30 min in 4% paraformaldehyde. The whole mount views of the interneurones are shown ventral-side up. In all cases the stimulated ChO is located on the right side of the drawing.

Recordings were made from cell bodies, axons and neuropile arborizations of interneurones in the anterior ventral median region of the ganglion (Fig. 2A). The interneurones were characterized according to their responses to stimuli applied to the receptor apodeme.

The behavioural state of a stick insect can be classed as either active or inactive (Bässler, 1983). The active state is characterized by activity of the fast extensor tibiae (FETi) motoneurone and the visible activity of the other leg joints, so the behavioural condition was monitored by extracellular recording of nerve F2 innervating the extensor tibiae muscle, using a modified hook electrode (Schmitz *et al.* 1988).

A special waveform generator (Hofmann & Koch, 1985) for trapezoidal movements was used for stimulating the ChO. With this apparatus it was possible to generate movements in which the values of the three movement parameters – position, velocity and acceleration – were controlled independently. To transform command voltages of the generator into precise mechanical motion of the apodeme, the signals were fed through a power amplifier connected to a low-frequency loudspeaker. Its coil carried a special paper cone, on which the apodeme clamp was mounted. A feedback system was used to ensure a precise transduction of the voltage to the position of the apodeme clamp. Thresholds for excitatory and inhibitory effects of the three parameters could be measured in detail by varying the movement parameters independently. Velocities for the different trapezoidal stimuli ranged from 0·05 to 27·8 mm s^{-1} (≈10 to ≈$5{\cdot}56\times10^{3}$

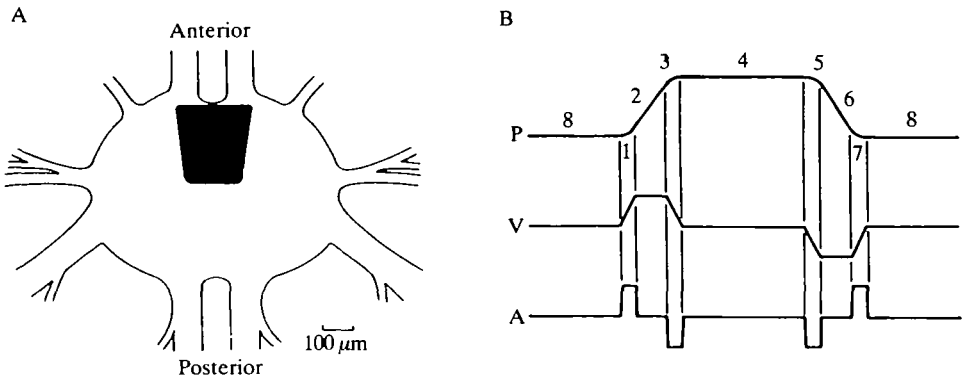

Fig. 2. (A) Recording region in the mesothoracic ganglion of *Carausius morosus*. View from the ventral side. (B) Phases of a trapezoidal stimulus. The first trace shows the position profile (P), the second one the velocity profile (V) and the third one the acceleration profile (A). The different phases are: (1) the start of elongation; the stimulus velocity (positive values) increases with positive acceleration; (2) the elongation phase at constant velocity; acceleration is zero during this phase; (3) the break phase of the elongation stimulus; the velocity decreases with negative acceleration; (4) the elongated state of the ChO (corresponding to a femur–tibia angle of 70°); (5) the start phase of relaxation; the velocity (negative values) increases with negative acceleration; (6) the relaxation phase at constant velocity; acceleration is zero (third trace); (7) the break phase of the relaxation stimulus; the velocity decreases with positive acceleration; (8) the relaxed state of the ChO, corresponding to a femur–tibia joint angle of 90°.

degrees s^{-1}), acceleration ranged from 0·3 to 39 700 mm s^{-2} (≈60 to ≈7·94×10^6 degrees s^{-2}).

It is obvious that parameter values of the different stimuli have influences on the latencies measured, because the thresholds of different receptor units are crossed after different stimulus durations, according to the different values of velocity and acceleration. Therefore, latencies between the stimulation events and the first effects in the interneurones are always noted in addition to the form of the stimulus, as described by velocity and acceleration.

All recordings were stored, together with position and velocity signals of the stimuli, extracellular (nerve F2) recording, current monitor and stimulus trigger signal, on magnetic tape (Racal Store 7DS) for later display and evaluation on a digital storage oscilloscope (Physirec by L. Neumann). An amplitude and peak window discriminator (designed by P. Heinecke, München) was used to convert spikes to TTL signals (0–5 V square-wave signals). Peristimulus-time histograms were generated using an Apple IIe microcomputer with a special interface (M. Spüler, in preparation).

Results

Results are based on recordings from 55 interneurones (49 intersegmental and 6

local) that were found to respond to stimulation of the ChO. Stainings of these interneurones exhibited more than 30 different anatomical patterns, of which some were found often (up to 14 times). Because of the large number of morphological types, I have classified the interneurones on the basis of reaction pattern to the defined ChO stimuli. All interneurones described here were at least partly (soma, axon or neuropile arborizations) located in the anterior median ventral part of the mesothoracic ganglion (Fig. 2). Physiologically, all the neurones were affected by at least one of the different receptor units of the femoral ChO. No investigation was made of whether these receptor units were connected monosynaptically or polysynaptically to the interneurones.

Definition of a physiological classification matrix for interneurones

The results are summarized in Table 1.

During trapezoidal stimulation of the ChO eight different stimulation phases were observed for the elongation and the relaxation direction (Fig. 2B), as defined by combinations of position, velocity and acceleration.

Only a minority of the characterized interneurones showed effects elicited by only one movement parameter (see Table 1). Most of the recorded interneurones showed responses to a combination of movement parameters (see Figs 13, 14). Hofmann *et al.* (1985) have already proposed a classification for the single sensory units in the ChO based on their response to position, velocity and acceleration stimuli. However, this classification scheme is not sufficient to describe effects of ChO stimulation on interneurones for two reasons. First, the abbreviations used by Hofmann *et al.* (1985) do not allow a unique description of all different effects that can be detected. Second, use of this classification implies a direct causality between distinct receptor units and the physiology of single interneurones.

In this paper I use a matrix system to describe all physiological types of interneurones. The matrix has the following features. (1) The induced effects of each of the eight phases of the trapezoidal stimulus (Fig. 2B) are accommodated in the matrix. (2) Excitatory and inhibitory effects are distinguished. (3) The matrix can be enlarged with further information if necessary, e.g. connections of the characterized interneurone.

The classification scheme is shown in Table 2. Each column represents one stimulus parameter of a trapezoidal stimulus (see legend of Fig. 2B). The first row contains the description of the effects of the stimulus parameters during elongation of the ChO, the second row does the same for relaxation. The numbers in the scheme (see Table 2) indicate the different phases marked in Fig. 2B. For example, effects of velocity input during an elongation stimulus (representing the response during phase 2 of the stimulus, Fig. 2B) would be noted in the first row in the second column. The results are recorded as follows. If a stimulus parameter has no effect, the corresponding matrix element carries a zero. Effects increasing the activity of interneurones, such as excitatory ones, are labelled 1, and effects decreasing activity, such as inhibitory ones, are labelled −1. Acceleration-induced effects were sometimes found to have long latencies (more than 25 ms). In some of

Table 1. *Summary of the physiological and morphological types of the characterized interneurones*

Effective stimulus parameter		Physiological type (matrix) P	V	A	Number	Morphological types	Additional effects
Position	E	1	X	X	5	4	Velocity
	R	−1	X	X			Acceleration
		−1	X	X	1	1	Velocity
		1	X	X			
Velocity		X	1	X	11	6	Position
		X	1	X			Acceleration
		X	1	X	3	3	Acceleration
		X	0	X			
		X	−1	X	18	5	Acceleration
		X	−1	X			
		X	−1	X	4	2	
		X	0	X			
		X	0	X	1	1	Acceleration
		X	−1	X			
Acceleration		X	X	1 (or 0)	12	8	
		X	X	1 (or 0)			

The first column represents a classification (see text) by the most effective stimulus parameters.

The second column shows the general physiological type of the interneurones collected in this class (only the first three columns of the matrix). Only the classifying parts relevant for the guideline are filled in, all other places in the matrices contain X. Neurones with acceleration-induced effects are clustered in only one class without differentiation of special response characteristics (see column 2).

The third column shows the number of recorded interneurones of the appropriate physiological type.

The fourth column shows the number of different morphological types found in each group. Each morphological type of interneurone shows the same soma location, primary neurite trace and similar main arborization structures and regions. Since neurones were classified according to their predominant reaction pattern, in two cases the same morphological type appears in different rows (see Figs 3A, 8A).

The last column presents additional effects of other stimulus parameters on interneurones of each group.

P, position; V, velocity; A, acceleration; E, elongation; R, relaxation. See text for further explanation.

these cases it was therefore not possible to define the acceleration phase of the stimulus that induced the effect on the recorded interneurone. Therefore, the classification scheme contains three columns (columns 3,4,5) for defining acceleration effects. Column 3 gives qualitative information about an effect elicited by acceleration in an elongation or relaxation stimulus. Usually the fourth and fifth

Table 2. *Matrix scheme for the physiological classification of the recorded interneurones*

	Position P	Velocity V	Acceleration A	Acc. start A_S	Acc. break A_B
Elongation	4	2	1,3	1	3
Relaxation	8	6	5,7	5	7

The numbers written in the matrix scheme belong to the eight phases of a trapezoidal stimulus shown in Fig. 2B (for further details see text).

columns contain information which describes the effect of the start (1,5 in Fig. 2B) or the break of the acceleration phase (3,7 in Fig. 2B).

The interneurones were grouped according to their main response characteristics (Table 1), and these characteristics are used in this paper as a guideline for the discrimination of the different physiological types of interneurones.

Interneurones with mainly position inputs

The signals of position-coding units of the ChO had a strong effect on six interneurones (six neurones, five morphological types, see Table 1); for example, the excitation level of phases 8 and 4 of the stimulus (Fig. 2B) differed markedly. Increased elongation of the ChO was found to have either increasing or decreasing effects on the static activity of these neurones.

In all six interneurones, position-induced effects from the ChO were accompanied by effects elicited by the dynamic part of the stimulus. Position was not the only stimulus parameter affecting these neurones. For example, Fig. 3B shows the reaction of an intersegmental interneurone (its morphology is shown in Fig. 3A) to elongation (joint-flexion) of the ChO from $-100\,\mu m$ ($\approx 110°$) to $+100\,\mu m$ ($\approx 70°$). The position change caused an increase in spike frequency (Fig. 3C). During the step of the stimulus from one position to the next, more-elongated one (Fig. 3B, asterisks), effects induced by the dynamic parameters of the elongation are visible in the interneurone response. In the interneurone shown in Fig. 4, relaxation (joint extension) of the ChO was correlated with an increasing static frequency of spiking. The other position-sensitive interneurones were also intersegmental ones.

Interneurones with velocity inputs

Velocity-dependent effects were characterized by their dependence on a velocity threshold that has to be crossed during the ramp phase of a trapezoidal stimulus (phases 2, 6; Fig. 2B). Recordings were made from 37 interneurones that responded mainly to velocity inputs from the ChO, but only very weakly or not at all to position input (Table 1).

The velocity of a stimulus carries a sign which depends on the stimulus direction (see Fig. 2B): in this paper, elongation ramps (joint flexion) are given positive velocities and relaxation ramps (joint extension) negative velocities.

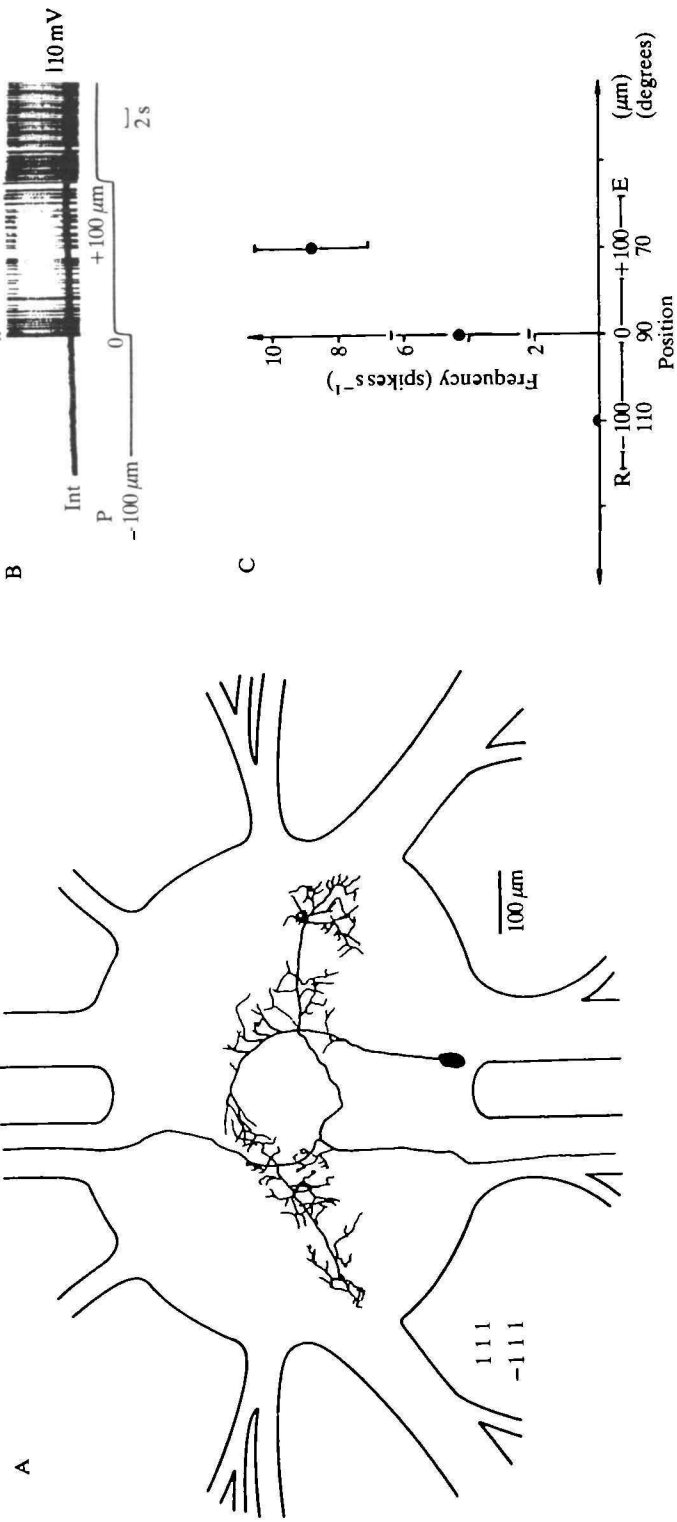

Fig. 3. (A) *Camera lucida* drawing of a mesothoracic intersegmental interneurone (stained with Lucifer Yellow) which responded to position signals from the ChO. The orientation of the ganglion is ventral-side up. The physiological type is shown. (B) Interneuronal response (Int) to stimulation of the ChO. The activity of the interneurone increased tonically with elongation. Phasic effects are visible during the transients of position change (marked by the asterisks). A position (P) of the receptor apodeme of −100 µm corresponds to a femur–tibia angle of about 110°; a position of +100 µm corresponds to an angle of about 70°. (C) Static frequency of the interneurone plotted against position of the ChO for three angles. Each point represents the mean frequency of 10 measurements with increased or decreased length of the ChO over a period of 1 s. Standard deviations (S.D.) are indicated.

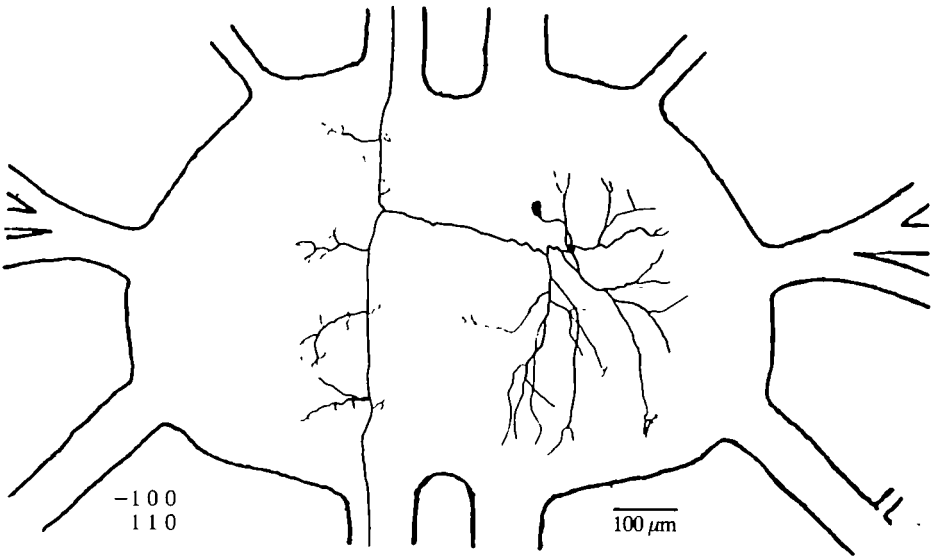

Fig. 4. Morphology of a mesothoracic intersegmental interneurone with position-dependent effects. The physiological type is shown. Relaxation of the ChO was correlated with increasing activity in the interneurone.

Interneurones with excitatory velocity inputs

The velocity of the stimulus was found to have strong excitatory effects on 14 recorded neurones. In three cases the interneurones were affected only by positive velocities (joint flexion; Fig. 2B, phase 2), and in 11 cases positive and negative velocities (joint flexion and joint extension; Fig. 2B, phases 2, 6) were shown to elicit spikes (Fig. 5A) in the interneurones.

For elongation stimuli (joint flexion), the velocity threshold for spike generation ranged from less than $+0{\cdot}1\,\mathrm{mm\,s^{-1}}$ (less than about $+20\,\mathrm{degrees\,s^{-1}}$) to $+9{\cdot}4\,\mathrm{mm\,s^{-1}}$ ($\approx+1{\cdot}9\times10^{3}\,\mathrm{degrees\,s^{-1}}$). Relaxation velocities (joint extension) induced spike generation over the same range [less than $-0{\cdot}1\,\mathrm{mm\,s^{-1}}$ ($\approx-20\,\mathrm{degrees\,s^{-1}}$) to $-9{\cdot}4\,\mathrm{mm\,s^{-1}}$ ($\approx-1{\cdot}9\times10^{3}\,\mathrm{degrees\,s^{-1}}$)]. Table 3 shows details of the analysis for 13 interneurones.

Fig. 5A,B shows typical activity of the interneurones affected by velocity input from the ChO. Plotting the mean frequency of action potentials during elongation (joint flexion) against stimulus velocity produced a nearly linear correlation in a log–log plot (Fig. 5C). The morphology of the corresponding interneurone is shown in Fig. 6. Both positive and negative velocities (joint flexion and extension) induced spikes in this interneurone, and velocities even smaller than $0{\cdot}1\,\mathrm{mm\,s^{-1}}$ ($\approx20\,\mathrm{degrees\,s^{-1}}$; see Table 3, no. 4) caused an increase in spike frequency. Ramps with a velocity of $+3{\cdot}2\,\mathrm{mm\,s^{-1}}$ ($\approx640\,\mathrm{degrees\,s^{-1}}$) and a high acceleration induced the first spike in this interneurone after a latency of 5·8 ms ($N=4$).

For elongation stimuli (positive velocity; joint flexion), the dependence of the response frequency on the stimulus velocity was compared for seven interneurones

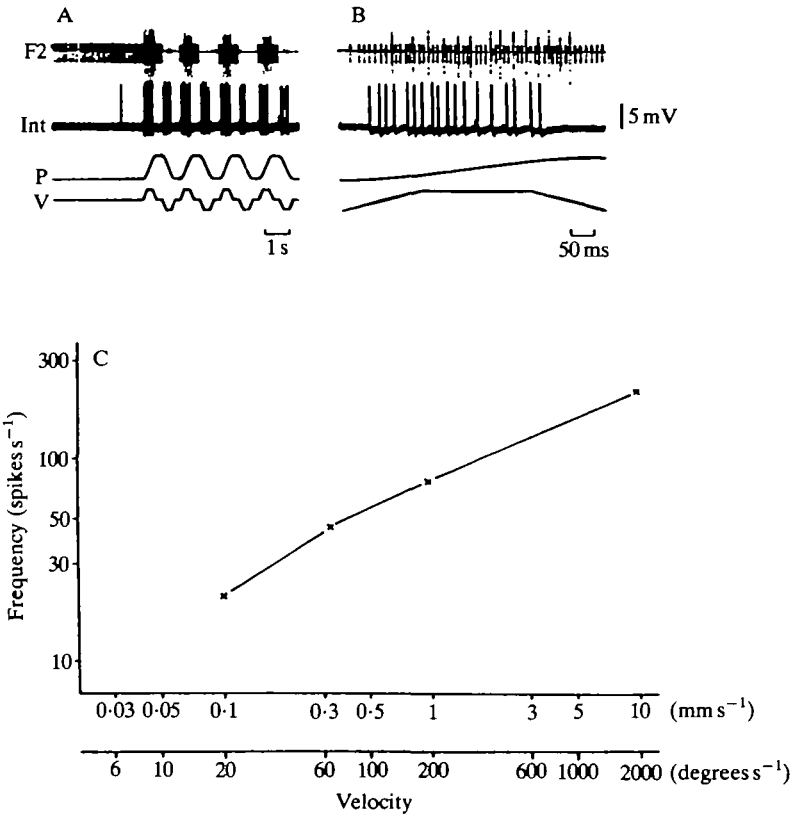

Fig. 5. Physiological properties of the interneurone shown in Fig. 6. (A) Response to trapezoidal stimulation of the ChO. (In all following figures elongation of the ChO is shown by an upward movement of the position trace, and corresponds to an angle change from 90° to 70° between the femur and the tibia; downward movement means a relaxation from 70° to 90°.) (B) Stimulation of the ChO with a stimulus velocity of $\pm 0{\cdot}1\,\mathrm{mm\,s^{-1}}$. The latency between the start of the ramp and the first spike in the interneurone contains the transduction time of the sensory signal and the time the stimulus needs to reach the threshold velocity to induce excitation in sensory cells and later on in interneurones. A and B are taken from different interneurones with the same physiological characteristics. (C) Plot of the mean frequency of action potentials *versus* stimulus velocity for the interneurone shown in Fig. 5 (Table 3, no. 2). The mean spike activity of three stimuli is averaged. F2, recording from nerve F2; Int, interneurone; P, position; V, velocity.

(Fig. 7; nos 1,2,4,5,6,10,13 of Table 3) of different morphological types, three of which are shown in Fig. 8. These interneurones showed an increasing mean frequency of spikes with an increase of stimulus velocity. The mean frequencies of these responses are comparable to the mean frequencies of velocity-sensitive receptor units in the ChO, shown by the area between the dashed lines in Fig. 7 (see Hofmann *et al.* 1985, fig. 6).

The single point at $+3{\cdot}2\,\mathrm{mm\,s^{-1}}$ ($\approx +640\,\mathrm{degrees\,s^{-1}}$) in Fig. 7 was recorded

Table 3. *Spike-initiating velocity thresholds*

Number	Threshold for elongation ($mm\,s^{-1}$)	Threshold for relaxation ($mm\,s^{-1}$)	Physiology P	V	A	A_S	A_B
1	$0<T_E<0{\cdot}1$	$-0{\cdot}1<T_R<0{\cdot}1$	0	1	1	1	0
			0	1	1	1	0
2	$0<T_E<0{\cdot}1$	$-0{\cdot}1<T_R<0$	1	1	0		
			−1	1	0		
3	+0·1	−0·1	0	1	0		
			0	1	0		
4	+0·1	−0·1	1	1	1		
			−1	1	1		
5	+0·1	−0·3	1	1	1		
			−1	1	1		
6	+0·3	−0·3	1	1	1		
			−1	1	1		
7	+0·3	−0·3	0	1	0		
			0	1	0		
8	+0·3	−0·3	0	1	1	1	0
			0	1	1	1	0
9	+0·3		0	1	1	1	0
			0	0	1	1	0
10	+0·3		0	1	0		
			0	0	0		
11	+1·0	−0·3	0	1	0		
			0	1	0		
12	+1·0		0	1	1		
			0	0	1		
13	+3·2	−3·2	0	1	1	1	0
			0	1	1	1	0

The physiological types of each neurone are shown in the last column. Neurones nos 4,5,6,8 and 12 have a similar morphological type, one is shown in Fig. 8A.

T_E, threshold for elongation; T_R, threshold for relaxation; P, position; V, velocity; A, acceleration; S, start; B, break; E, elongation; R, relaxation.

from an intersegmental interneurone of special interest (Fig. 9; Table 2, no. 13): velocity-dependent spike generation only appeared for a single velocity value (Fig. 9B,C). Trapezoidal stimuli at higher velocity than $+3{\cdot}2\,mm\,s^{-1}$ induced only one or two spikes during the start phase of stimulation (Fig. 9D,E). Velocity values lower than $+3{\cdot}2\,mm\,s^{-1}$ had a similar effect (not shown). The spikes were elicited by acceleration-dependent excitatory effects in the interneurone (for tests of acceleration input see Figs 14 and 17). The acceleration threshold for spike initiation was $+5\,mm\,s^{-2}$ ($\approx+1\times10^3$ degrees s^{-2}), and the first stimulus-induced spike showed a latency of 18·9 ms (S.D. = 1·8, $N = 7$) for a stimulus with a velocity

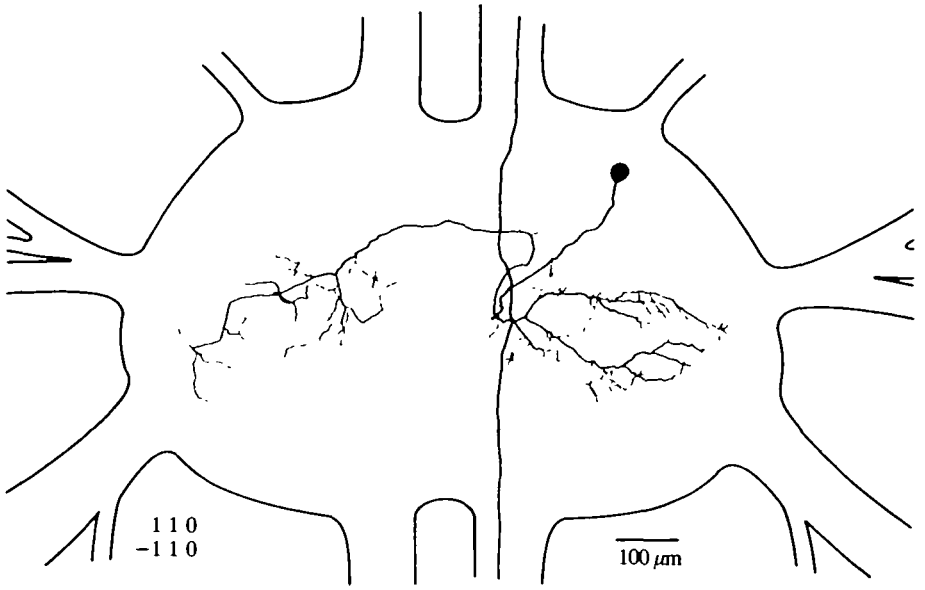

Fig. 6. Morphology and physiological type of a mesothoracic intersegmental interneurone with velocity-dependent responses (for physiology see Fig. 5; Table 3, no. 2).

of $+3{\cdot}2\,\mathrm{mm\,s^{-1}}$ ($\approx+640\,\mathrm{degrees\,s^{-1}}$) and acceleration of $\pm196\,\mathrm{mm\,s^{-2}}$ ($\approx\pm3{\cdot}9\times10^{5}\,\mathrm{degrees\,s^{-2}}$).

Additional effects of acceleration or position signals were shown by several other interneurones with velocity input. One morphological type of interneurone, of which nine examples were found (examples: Table 3, nos 4,5,6,8,12; Table 5, nos 1,2), gave mostly excitatory responses to velocity signals for both stimulus directions and also showed different combinations of effects dependent on position or acceleration. In two cases, no velocity-induced response was found (Table 5, nos 1,2); in one case (Table 3, no. 12), only positive velocities were effective; and in another, position was the main effective stimulus parameter (Fig. 3). The morphology of one of the interneurones with strong velocity-dependent effects combined with position-dependent effects is shown in Fig. 8A (compare Fig. 3, which is similar morphologically).

The soma of each of these interneurones was located between the entrances of the two posterior connectives on the ventral side of the ganglion, slightly ipsilateral to the stimulated ChO. The primary neurite left the soma ipsilaterally. Nearly in the middle of the ganglion, the neurite separated into three branches; the one with the largest diameter crossed the midline of the ganglion. On this side the neurite formed two branches which left the ganglion to the anterior and posterior side through the contralateral connectives.

Both elongation (joint flexion) and relaxation (joint extension) of the ChO induced an increase in spike frequency (Fig. 10A) in this interneurone (Fig. 8A, Table 3, no. 4). An increase in velocity, whether positive or negative, was

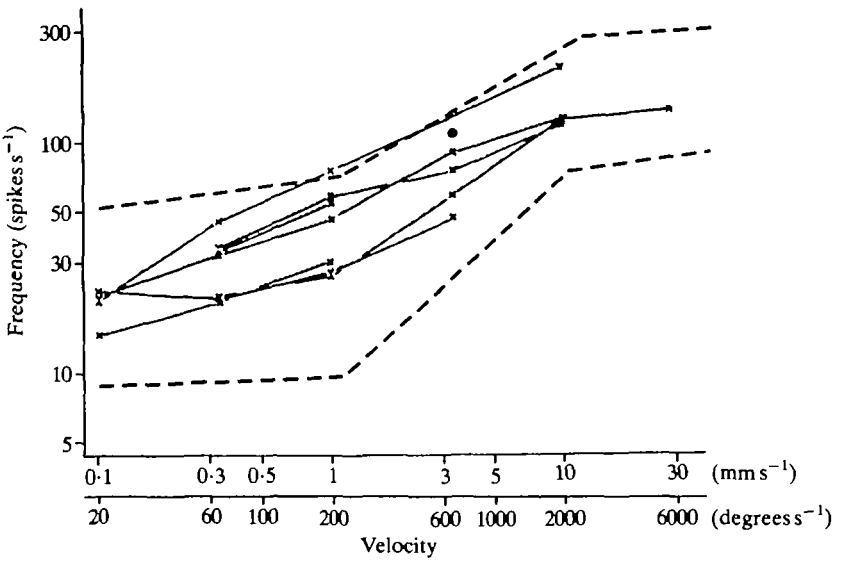

Fig. 7. Comparison of responses of different interneurones to velocity input (Table 3, nos 2,10,5,4,6,1, from top to bottom, at a velocity of +1 mm s^{-1}). The thresholds of the interneurone in the third curve from the top are not given in Table 3. The single dot belongs to neurone 13 in Table 3. Mean frequency of action potentials is plotted *versus* velocity of the stimulus during elongating apodeme movement. Every line corresponds to one interneurone. The area between the dashed lines denotes the range of response characteristics of the sensory units of the ChO (Hofmann *et al.* 1985)

correlated with an increase in mean frequency of action potentials in the interneurone (Fig. 10B). A latency of 13·4 ms ($N = 4$) was measured between the start of an elongation stimulus and the first spike for a stimulus velocity of +10 mm s^{-1} ($\approx +2\times10^3$ degrees s^{-1}). During the static phase of the trapezoidal stimulation (phases 4 and 8 in Fig. 2B) the interneurone showed slight spontaneous activity. This activity depended on the position of the ChO. Comparing the neuronal activity for two positions (joint-angles) – relaxed (0 μm; about 90°) and elongated (+100 μm; about 70°) – averaged over a period of 90 s, tonic activity of the interneurone was higher in the more elongated position (0 μm: 1·3 Hz; +100 μm: 3·0 Hz).

Interneurones with inhibitory velocity inputs

Inhibitory effects of velocity signals were found in 23 interneurones: five showed inhibitory effects during positive or negative velocities; 18 during both velocity directions.

Several interneurones that were strongly hyperpolarized during elongation and

Fig. 8. Morphology and physiological type of different interneurones in the mesothoracic ganglion responding to velocity signals from the ChO. Excitation thresholds are given in Table 3: A, no. 4; B, no. 11; C, no. 10.

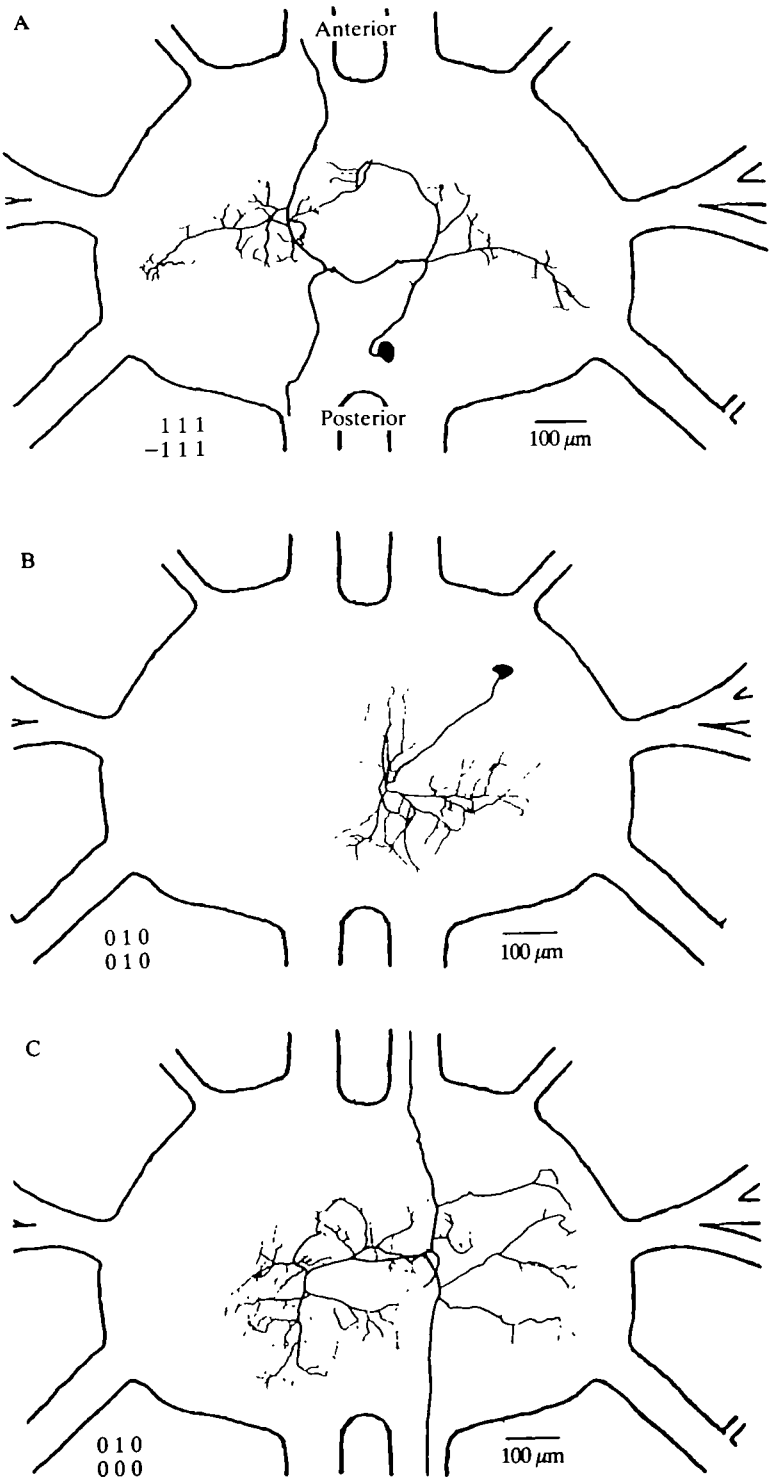
A
Anterior
Posterior
1 1 1
−1 1 1
100 µm
B
0 1 0
0 1 0
100 µm
C
0 1 0
0 0 0
100 µm

Fig. 8

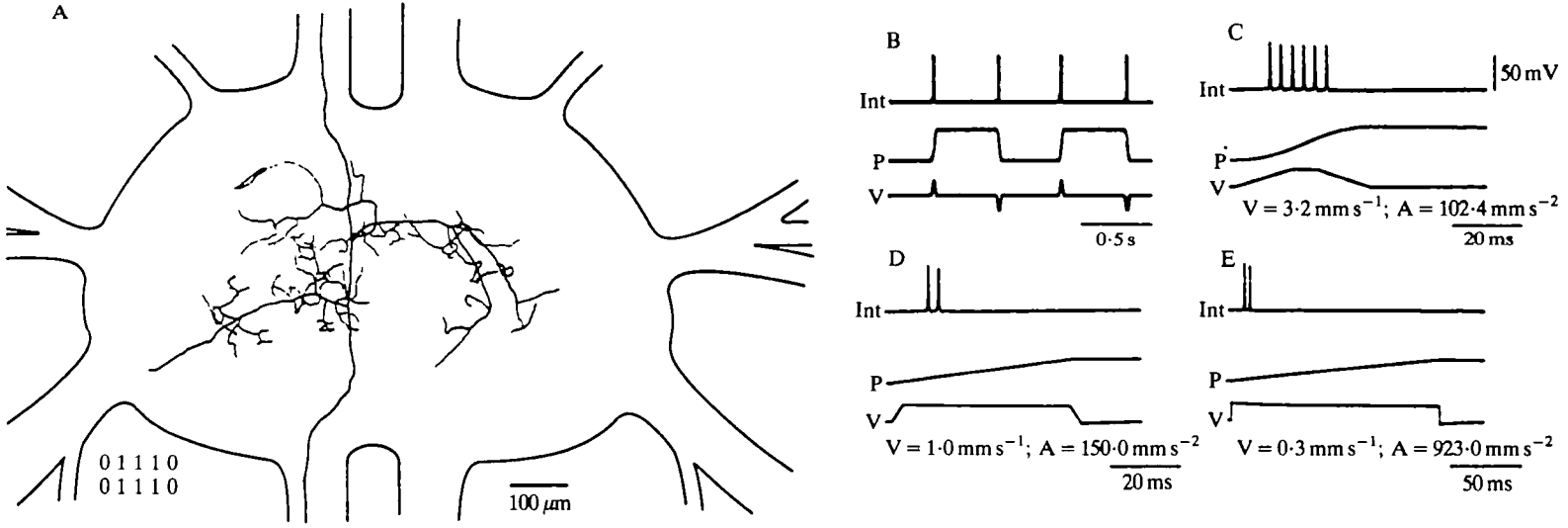

Fig. 9. (A) Arborizations of an intersegmental interneurone. This interneurone was stimulated by ChO stimulation (Table 3, no. 13). The soma location is unknown. Properties of the interneurone: (B) effects of elongation and relaxation stimuli on the interneurone; (C) trapezoidal stimulation at a velocity of $3{\cdot}2\,mm\,s^{-1}$. (D,E) Effects of stimuli with decreased velocity ($\pm1{\cdot}0$, $\pm0{\cdot}3\,mm\,s^{-1}$) and increased acceleration value (±150, $\pm923\,mm\,s^{-2}$). P, position; V, velocity; Int, interneurone.

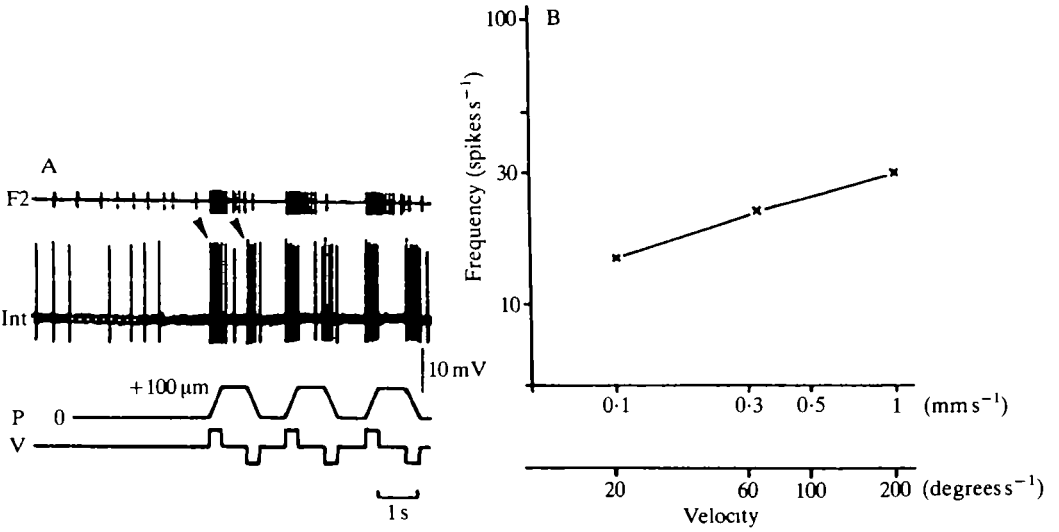

Fig. 10. Properties of the interneurone shown in Fig. 8A. (A) The interneurone was excited by position transients. (B) Plot of the mean frequency of action potentials during elongation stimuli *versus* velocity of stimulation. The mean spike activity of four ramps is averaged. F2, recordings from nerve F2; Int, interneurone; P, position; V, velocity.

relaxation stimuli (Fig. 11A) belonged to a group of descending interneurones which had somata clustered in the anterior median lateral part of the ganglion, ventrally located, contralateral to the stimulated ChO (A. Büschges, unpublished results). The primary neurite left the soma by crossing the midline of the ganglion and arborized mainly ipsilateral to the ChO. All neurones stained (11 successful stainings, 14 recordings; Table 4, nos 1–11) sent one prominent branch to the site where the nervus cruris enters the ganglion. Each of the axons then left the ganglion through the ipsilateral connective. Owing to the long connectives in *Carausius morosus*, the dye did not spread into the next ganglion, so projection regions in the posterior ganglia are not yet known.

All the recorded interneurones were tonically active with fluctuating activity (Fig. 11B). Stimulation of the ChO, once a distinct positive and negative velocity 'threshold' had been reached, led to a total inhibition of activity in these interneurones during the stimulus and a remarkable hyperpolarization was visible (Fig. 11B). Plotting the hyperpolarization during stimulation against the stimulus velocity for one interneurone of this type (Fig. 12A; detailed thresholds for this neurone are given in Table 4, no. 1), showed an increasing hyperpolarization with increasing velocity, for both positive (joint flexion) and negative velocities (joint extension; Fig. 11C,D; Fig. 12A). (It must be taken into account that the amplitude of IPSPs depends on the value of the resting potential and on the value of the reversal potential.) The amount of hyperpolarization during either elongation or relaxation was not correlated with the amount of acceleration at the

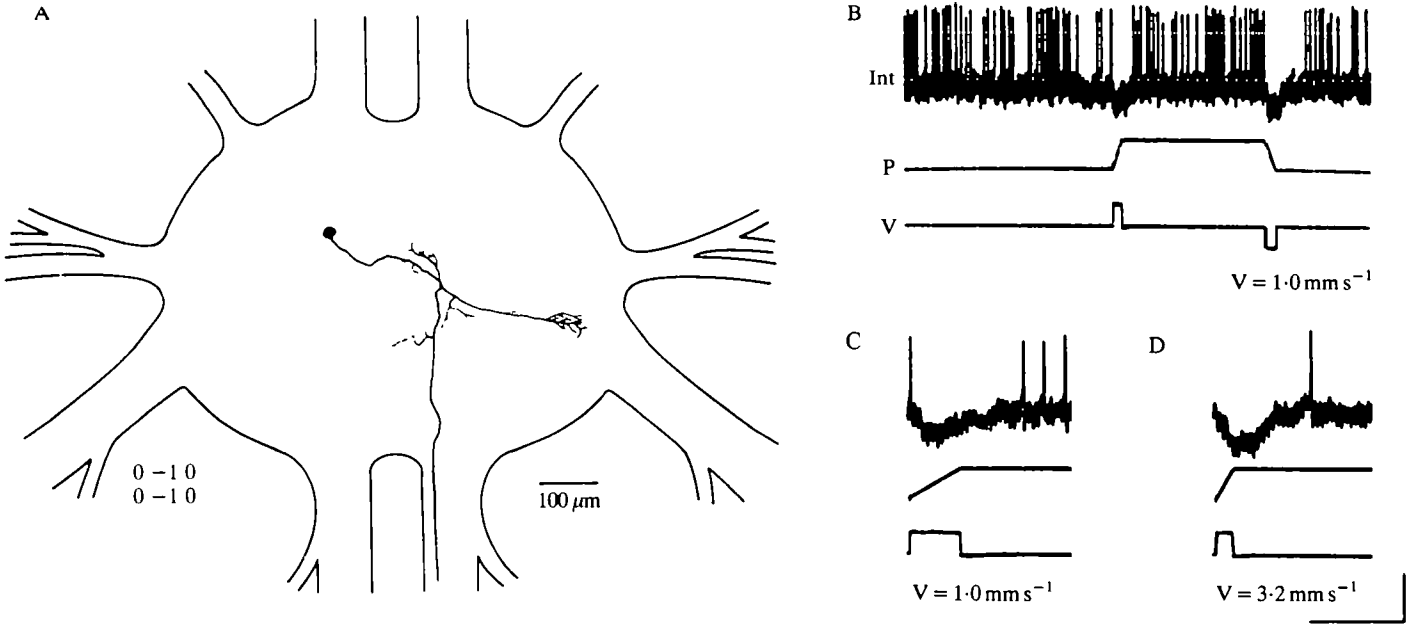

Fig. 11. Properties of a descending intersegmental interneurone in the mesothoracic ganglion with velocity-dependent effects. (A) Morphology and physiological type. This interneurone is mentioned in Table 4, no. 1. (B) Response characteristics of this interneurone to rampwise stimulation of the ChO. Elongation and relaxation stimuli induced a strong inhibition in the interneurone, shown by a soma recording. (C,D) Effects of ChO stimulation at two different velocities (calibration bars, vertical 1 mV; horizontal B, 2 s; C,D, 0·1 s). P, position; V, velocity; Int, interneurone.

Table 4. *Velocity thresholds for total inhibition of tonic activity during the stimulus and acceleration thresholds for spike initiation*

	Inhibition threshold		Excitation threshold Elongation		Relaxation						
	Elongation	Relaxation	Start	Break	Start	Break	Physiology				
Number	($mm\,s^{-1}$)		($mm\,s^{-2}$)				P	V	A	A_S	A_B
1	+0·1	−0·1					0	−1	0		
							0	−1	0		
2	+0·3	−0·3					0	−1	0		
							0	−1	0		
3	+0·3	−0·3					0	−1	0		
							0	−1	0		
4	+0·3	−1·0					0	−1	0		
							0	−1	0		
5	+1·0	−0·1					0	−1	0		
							0	−1	0		
6	+0·1	−0·1	+5·9	−5·9	−5·9	+5·9	0	−1	1	1	1
							0	−1	1	1	1
7	+0·1	−0·3	+3·1	−3·1	−3·1	+3·1	0	−1	1	1	1
							0	−1	1	1	1
8	+0·3	−0·3	+29·5	−29·5	−29·5	+29·5	0	−1	1	1	1
							0	−1	1	1	1
9	+0·3	−0·3	+5·0	−19·7	−5·0	+10·3	0	−1	1	1	1
							0	−1	1	1	1
10	+1·0	−1·0	+148·0	−148·0	−148·0	+148·0	0	−1	1	1	1
							0	−1	1	1	1
11	+1·0	−1·0	+148·0	−148·0	−148·0	+148·0	0	−1	1	1	1
							0	−1	1	1	1
12	+0·1	−0·1					0	−1	0		
							0	−1	0		
13	+0·3	−0·3					0	−1	0		
							0	−1	0		
14	+0·3	−0·3					0	−1	0		
							0	−1	0		
15	+3·2	−3·2					0	−1	0		
							0	−1	0		

Neurones nos 1–11 belong to a group of similar morphological type (see Figs 11, 13). For abbreviations, see Table 3.

beginning and end of the stimulus (Fig. 12B). The velocity thresholds for total inhibition are shown in Table 4. Interneurones nos 1–5 in Table 4 belonged to this physiological type. Shortest latencies between the onset of a stimulus and a visible hyperpolarization were about 10 ms.

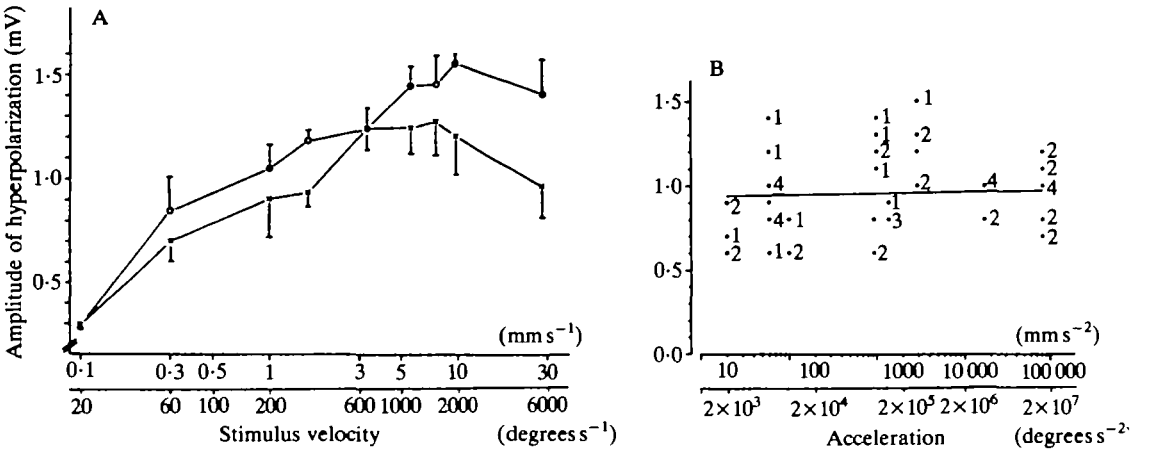

Fig. 12. (A) Plot of the amplitude of hyperpolarization *versus* stimulus velocity for elongation and relaxation stimuli (x, elongation; o, relaxation, Table 4, no. 1). The standard deviations are shown ($N = 5$–18). (B) Plot of the amplitude of inhibition during elongation stimuli *versus* acceleration of the stimuli. The numbers indicate the number of values in this point. Regression line is $x = 0{\cdot}9 \times 10^{-6} y$, Regression coefficient = 0·009.

The other six analysed interneurones (Table 4, nos 6–11) of this morphological type showed not only inhibition by velocity signals from the ChO, but also excitation by acceleration signals. The main characteristics of the morphology of these interneurones were similar to those of the interneurones receiving only inhibitory velocity effects (Fig. 13; no. 9 of Table 4). Velocity signals from the ChO had the same effects on these interneurones as those described above, causing total inhibition of activity above a certain threshold. The thresholds for inhibition varied over a wide range of values [$\pm 0{\cdot}1$ ($\approx \pm 20$ degrees s^{-1}) to $\pm 3{\cdot}2$ mm s^{-1} ($\approx \pm 640$ degrees s^{-1})]. Fig. 14 gives an example of such a neurone (Table 4, no. 9). Stimulating the ChO at a velocity of $\pm 0{\cdot}3$ mm s^{-1} [$\approx \pm 60$ degrees s^{-1}; acceleration $\pm 5{\cdot}0$ mm s^{-2} ($\approx \pm 1 \times 10^3$ degrees s^{-2})] caused a strong inhibition (Fig. 14A,B). Trapezoidal elongation (joint flexion) stimuli with the same velocity ($\pm 0{\cdot}3$ mm s^{-1}) but at an increased acceleration ($\pm 10{\cdot}3$ mm s^{-2}; $\approx \pm 2{\cdot}06 \times 10^3$ degrees s^{-2}) induced a slight depolarization in the interneurone at the upper edge of the ramp (Fig. 14C). For stimuli with an acceleration of $\pm 19{\cdot}7$ mm s^{-2} ($\approx \pm 3{\cdot}94 \times 10^3$ degrees s^{-2}) every break phase of the stimulus induced a spike (Fig. 14D). Therefore, the acceleration in the break phase (Fig. 2B, phase 3) excited the interneurone during hyperpolarization induced by the velocity inputs. The same effect was obvious for relaxation phases (joint extension) with an acceleration of $\pm 19{\cdot}7$ mm s^{-2} (Fig. 14E) as well as for the start phases of elongation and relaxation (Fig. 14B–E). Acceleration-induced spikes occurred with a latency of 17·5 ms (S.D. = 3·1, $N = 8$) for elongation ramps and 15 ms (S.D. = 2·4, $N = 8$) for relaxation ramps after onset of the stimuli. Thresholds for excitation by acceleration differed for different neurones. They

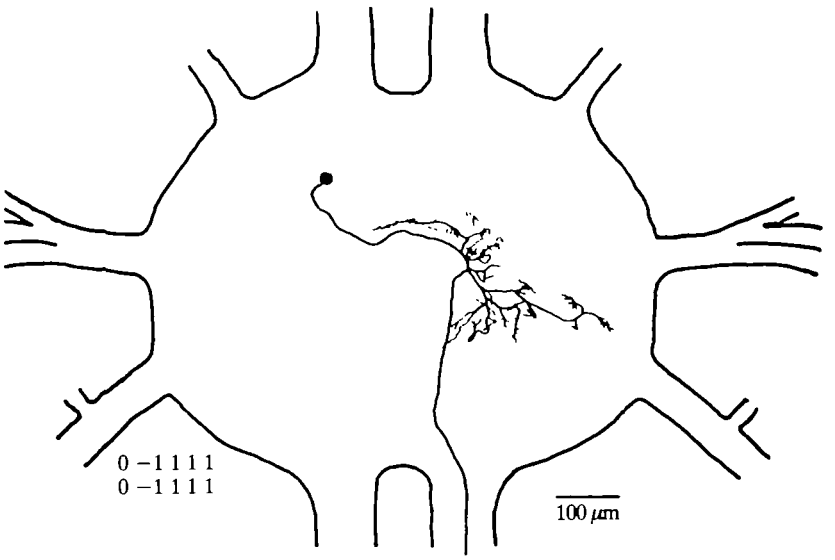

Fig. 13. The morphology and physiological type of a descending mesothoracic interneurone which showed inhibitory and excitatory responses induced by ChO stimulation (Table 4, no. 9). The morphology was similar to that of the interneurone whose properties are shown in Fig. 12.

ranged from $\pm 3{\cdot}1\,\mathrm{mm\,s^{-2}}$ ($\approx \pm 620\,\mathrm{degrees\,s^{-2}}$) to $\pm 148\,\mathrm{mm\,s^{-2}}$ ($\approx \pm 2{\cdot}96 \times 10^3\,\mathrm{degrees\,s^{-2}}$).

Interneurones with excitatory acceleration inputs

Effects that were induced by acceleration signals from the ChO were characterized by their dependence on a distinct acceleration threshold during the appropriate acceleration phase of a stimulus. Several interneurones were excited only by acceleration-dependent inputs from the ChO (Table 1). Acceleration-induced effects were always found to be excitatory.

A typical example of an acceleration response is shown in Fig. 15. Apart from occasional spikes, this interneurone was not spontaneously active (Fig. 15A). Stimulating the ChO at a given velocity, but with increasing acceleration values (Fig. 15B,C) at first caused spike generation in the interneurone during the relaxation phases (joint extension) of the stimuli. When stimuli at an acceleration of about twice as high ($\pm 5\,\mathrm{mm\,s^{-2}}$; $\approx \pm 1 \times 10^3\,\mathrm{degrees\,s^{-2}}$) were applied, elongation stimuli (joint flexion) elicited spikes as well (Fig. 15D). In this interneurone, spikes were induced by the start phases of the ramps (Fig. 15E) for elongation as well as for relaxation (no. 1, Table 5). Excitation thresholds for acceleration differed over a wide range of values, from (±)0·002 to (±)$39{\cdot}7\,\mathrm{m\,s^{-2}}$ ($\approx$ from 400 to $7{\cdot}9 \times 10^6\,\mathrm{degrees\,s^{-2}}$; Table 5), but were constant for a particular neurone. Neurones that were affected only by acceleration were all interganglionic (e.g. Fig. 16, Table 5, nos 6,8).

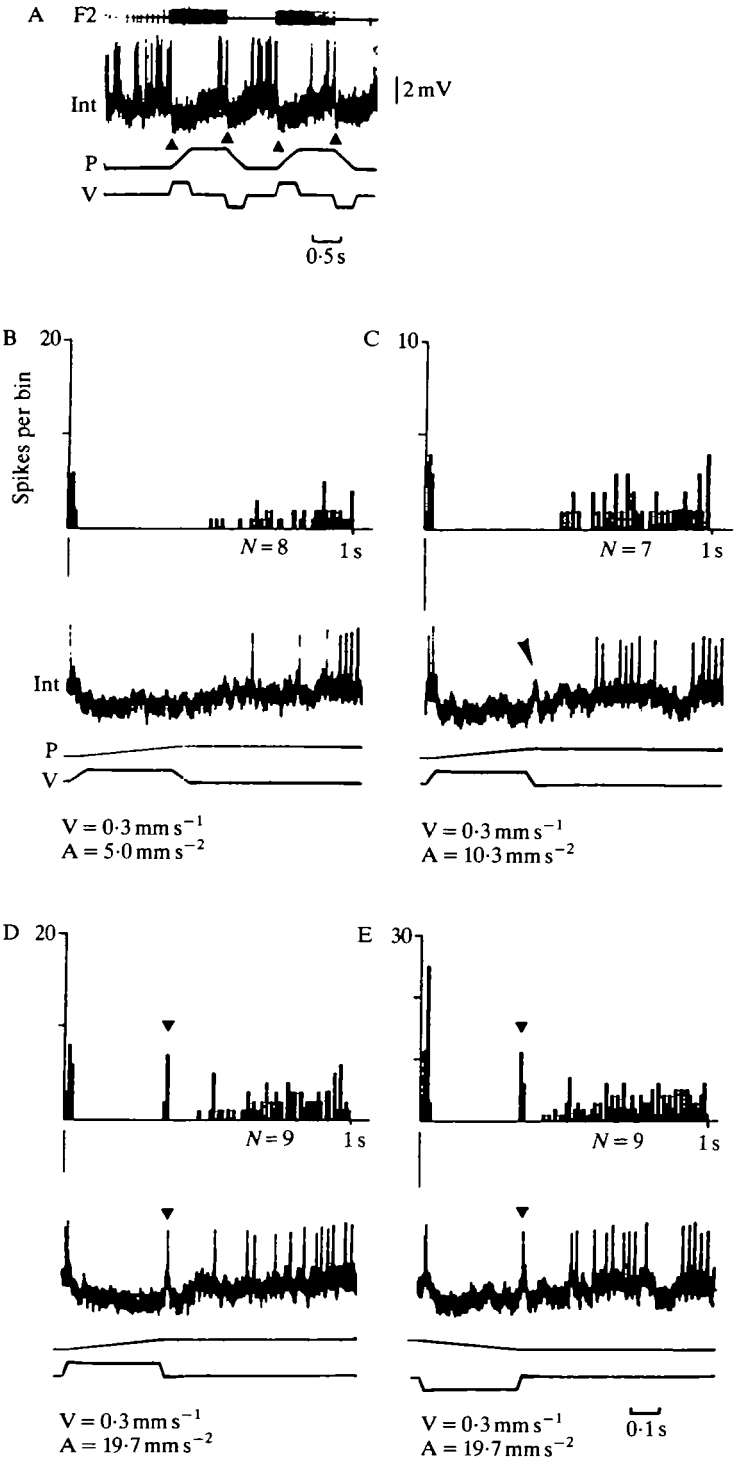

Fig. 14

Fig. 14. For legend see p. 104

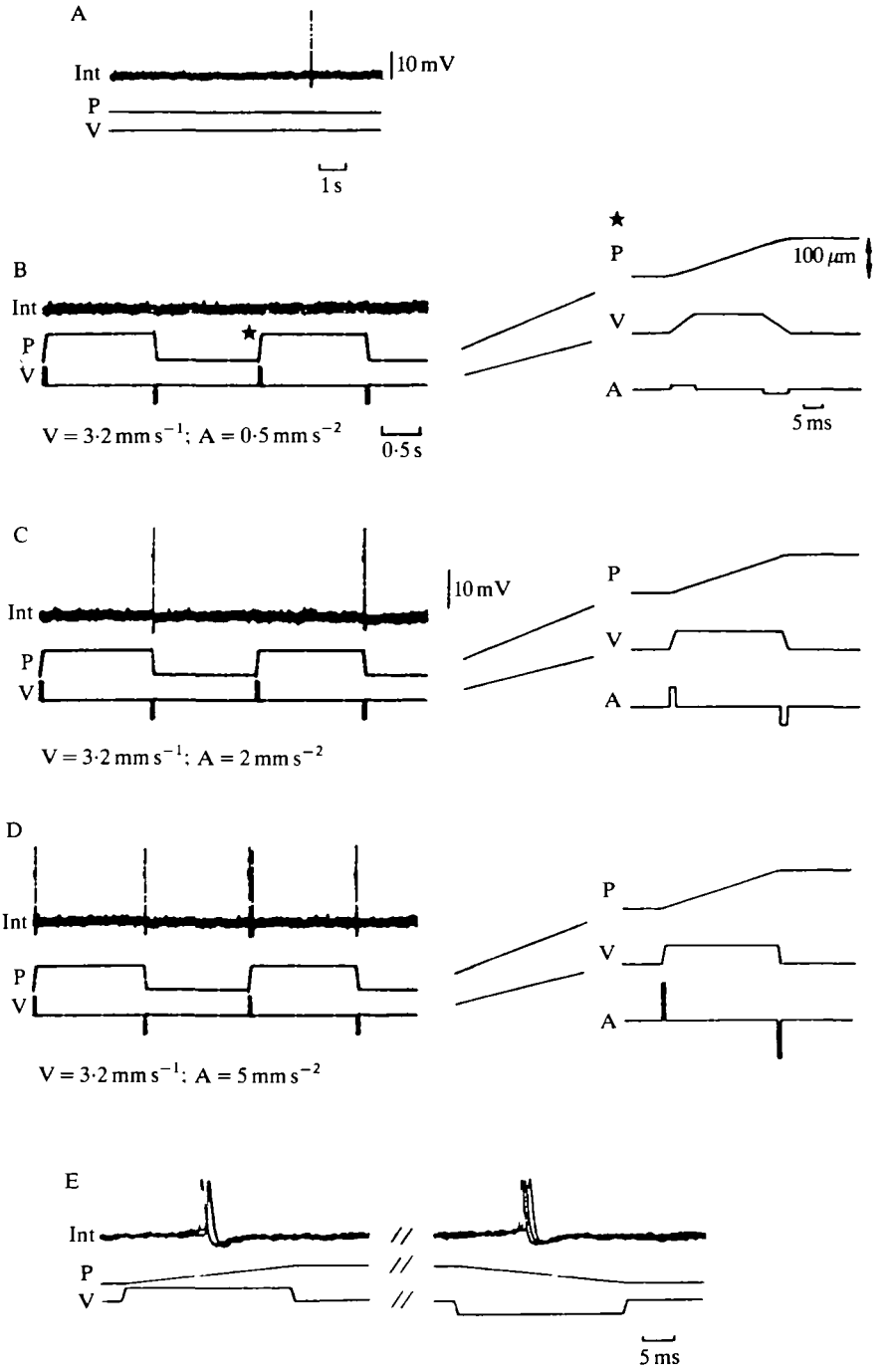

Fig. 15

Fig. 15. For legend see p. 104

Fig. 14. Properties of the interneurone shown in Fig. 13. (A) Rampwise stimulation of the ChO induced a strong inhibition in the interneurone (marked by the arrowheads). (B,C,D) Effects of elongation stimuli at a given velocity but increasing acceleration. (E) Effects of relaxation ramps. P, position; V, velocity; Int, interneurone.

Fig. 15. Physiological properties of an intersegmental interneurone with excitatory acceleration-dependent responses (Table 5, no. 1). (A) Activity of the interneurone without stimulation of the ChO. (B) Stimulation of the ChO at an acceleration of $\pm 0{\cdot}5\,mm\,s^{-2}$. On the right-hand side is the detailed structure of every applied stimulus. (C) Effects of increased acceleration ($\pm 2\,mm\,s^{-2}$) of the start and break phases. (D) Effect of a further increase of acceleration ($\pm 5\,mm\,s^{-2}$). (E) Expanded view of the stimuli shown in D (three traces superimposed; for details see text). A, acceleration; V, velocity; P, position; Int, interneurone.

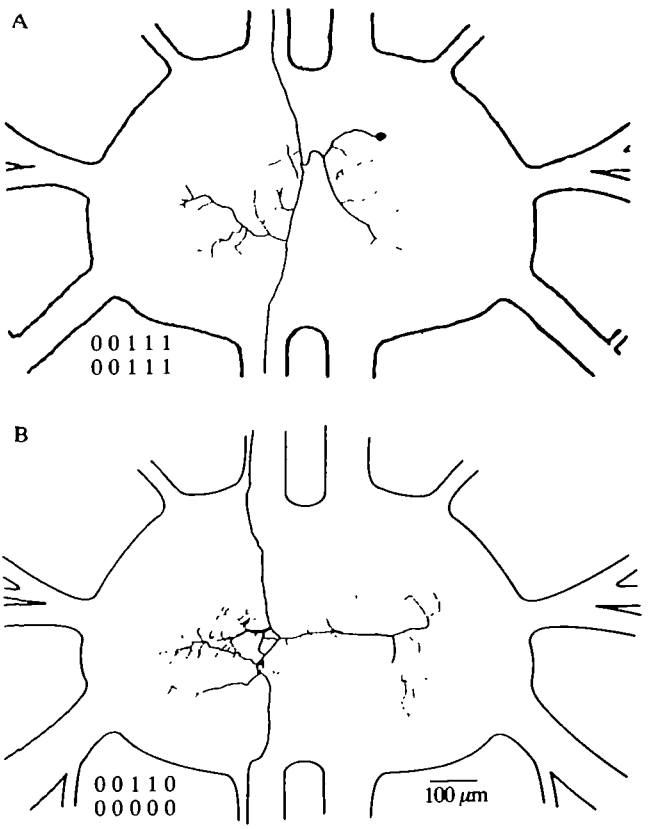

Fig. 16. Morphology and physiological type of two interneurones affected by acceleration signals from the ChO: (A) Table 5, no. 8; (B) Table 5, no. 6.

Table 5. *Acceleration thresholds for spike initiation*

Number	Threshold for elongation ($m s^{-2}$)	Threshold for relaxation ($m s^{-2}$)	Physiology P	V	A	A_S	A_B
1	+0·005	−0·002	0	0	1	1	0
			0	0	1	1	0
2	0·005	0·005	0	0	1		
			0	0	1		
3	+0·01	−5·9	0	0	1	1	0
			0	0	1	1	0
4		−0·15	0	0	0	0	0
			0	0	1	1	0
5	±0·2	±0·9	0	0	1	1	1
			0	0	1	1	1
6	+0·3		0	0	1	1	0
			0	0	0	0	0
7	+0·5	−0·15	0	0	1	1	0
			0	0	1	1	0
8	±1·4	±1·4	0	0	1	1	1
			0	0	1	1	1
9	2·8	13·5	0	0	1		
			0	0	1		
10	8·5	8·5	0	0	1		
			0	0	1		
11	39·7	39·7	0	0	1		
			0	0	1		

The sign of the acceleration threshold depends on the inducing acceleration phase (see Fig. 2B).

The physiological type of every interneurone is also shown.

Neurones 1 and 2 belong to the same morphological type as nos 4,5,6,8 and 12 in Table 3 (see Figs 3, 8A). The morphology of neurone 5 is similar to that of nos 1–11 in Table 4 (see Figs 11, 13). The arborizations of neurones 9, 10 and 11 belong to a common morphological type, not shown.

Eight interneurones were excited by the start phase (Fig. 2B, phases 1 and 5) of a ramp (examples: Table 5, nos 1,3,4,5,6,7,8); some of them by the break phase as well (Fig. 2B, phases 3 and 7; Table 5, nos 5,8). Detailed analyses failed for four interneurones (Table 5, nos 2,9,10,11) because the latencies were longer than the adequate stimulus duration. No interneurones, not even those with additional acceleration effects, were found to be affected only by the break phase of a stimulus, either for elongation or for relaxation.

Interneurones with inhibitory velocity inputs and with output effects on the slow extensor tibiae motoneurone (SETi)

Three local interneurones were found to be located mainly in the anterior part

Fig. 17. Properties of a local mesothoracic interneurone with inhibitory inputs induced by ChO stimulation and with excitatory connections to the SETi motoneurone. (A) Morphology and physiological type. (B) Effect of current injection in the interneurone. (C) Effect of ChO stimulation on the interneurone. (D) 10 elongation events superimposed. No spike occurred during the ramp (see Fig. 16). (E) Comparison of SETi activation by elongation of the ChO for two situations: interneurone depolarized (I = 5 nA), interneurone not depolarized. F2, recording from nerve F2, Int, interneurone; P, position.

of the ganglion (Fig. 17A). The somata lay in the anterior lateral region of the ganglion contralateral to the stimulated ChO, and the primary neurites crossed the midline and arborized ipsilateral to the stimulated ChO.

In all three recordings the interneurones were tonically active. Elongation of the ChO had a decreasing effect of variable strength on the activity of the interneurones. In no recording did the interneurones show any spikes during elongation ramp stimuli (joint flexion) of the ChO with velocity values above $+0{\cdot}3\,\mathrm{mm\,s^{-1}}$ ($\approx+60\,\mathrm{degrees\,s^{-1}}$; Fig. 17C,D). In two recordings it could be shown that this was due to a hyperpolarization by velocity signals from the ChO; the amount of hyperpolarization increased with increasing velocity. Elongation stimuli [velocity $+3{\cdot}2\,\mathrm{mm\,s^{-1}}$ ($\approx+640\,\mathrm{degrees\,s^{-1}}$), acceleration $\pm488\,\mathrm{mm\,s^{-2}}$ ($\approx\pm9{\cdot}7\times10^{5}\,\mathrm{degrees\,s^{-2}}$)] induced an inhibition in the example shown in Fig. 18 with a latency of 16·7 ms ($N = 4$). These neurones were not affected by relaxation stimuli (Fig. 17C).

Depolarization of these interneurones by current injection induced a tonically increased activity in the SETi motoneurone (Fig. 17B). A combination of depolarization of the interneurone and stimulation of the ChO elicited an increased activity of the SETi motoneurone during the resistance reflex (Fig. 17E). No investigation was made of whether this effect was only based on a higher activity of the SETi motoneurone, or whether the characteristics of the resistance reflex were changed. During activity of the animal the recorded interneurones were active with high discharge rates (more than 30 Hz). There was no effect of ChO stimulation detectable in the interneurones in this situation.

This type of interneurone was the only one which, when driven by current injection, influenced the discharging rate of one of the extensor motoneurones. No other neurones which could be driven by current injection (35 of the remaining 52 neurones) influenced the discharge rate of the motoneurones innervating the extensor tibiae muscle.

Discussion

The interneurones described here show a variety of responses to ChO stimulation and include responses to all three movement parameters: position, velocity and acceleration.

The physiology of all the recorded interneurones has been described by using a distinct range of parameter values (see Materials and methods). It cannot b

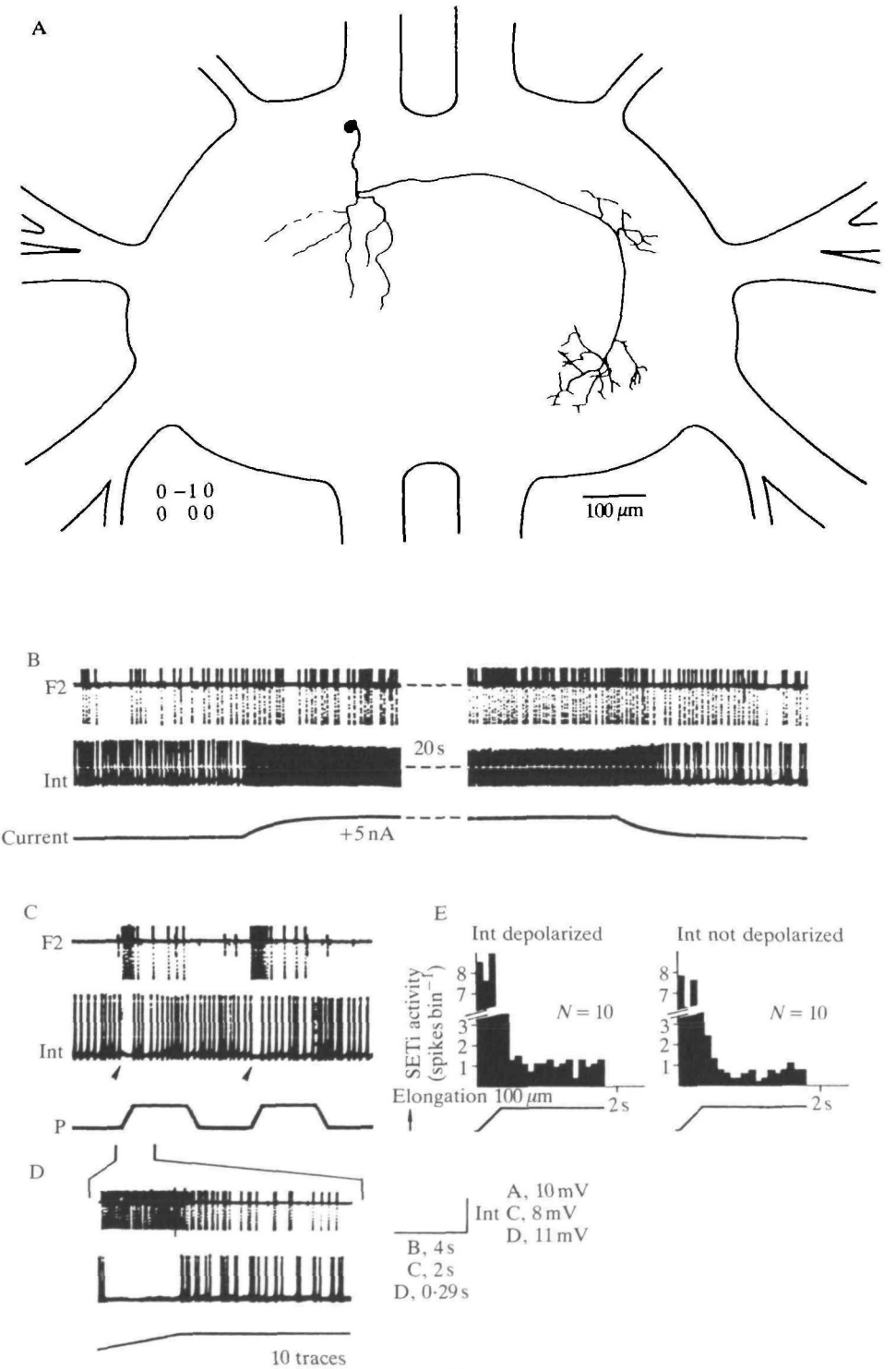
A
0 −1 0
0 0 0
100 μm
B
F2
Int
20 s
Current
+5 nA
C
F2
Int
P
D
10 traces
E
Int depolarized
Int not depolarized
SETi activity (spikes bin⁻¹)
8
7
3
2
1
N = 10
N = 10
Elongation 100 μm
2 s
2 s
A, 10 mV
Int C, 8 mV
D, 11 mV
B, 4 s
C, 2 s
D, 0·29 s

Fig. 17

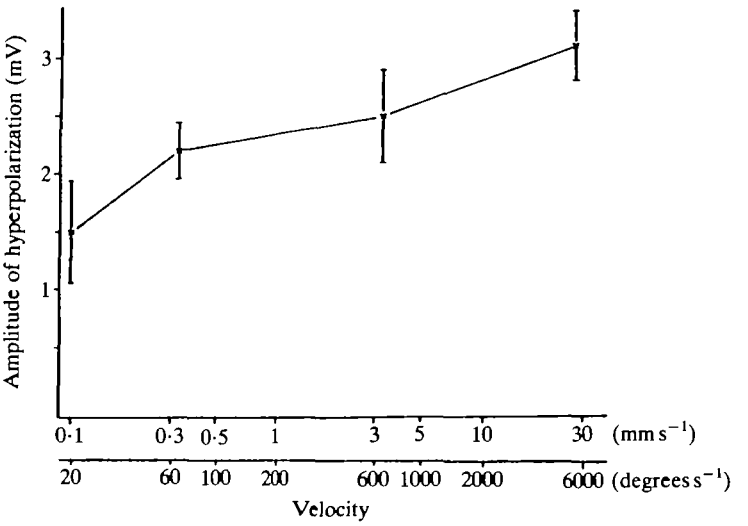

Fig. 18. Amplitude of hyperpolarization *versus* velocity of the elongation stimulus ($N = 10$–13). The data are taken from a recording (soma recording) of the same type of interneurone as that shown in Fig. 17. ±S.D. is indicated.

excluded that the physiological characteristics of these interneurones may be different in response to stimuli differing strongly from the ranges used here and in response to inputs from other sense organs changing their basic activity. This is also true for effects of range-fractionation, described by Hofmann *et al.* (1985) for sensory units in the ChO.

In these experiments no interneurone was found to be affected only by position signals from the ChO. Additional effects of velocity or acceleration or both always accompanied the position-induced effects.

Velocity-induced effects were either excitatory or inhibitory. Some interneurones were affected by the velocity input in only one stimulus direction, but most of the recorded interneurones were affected by both elongation and relaxation velocity. Excitatory effects elicited spikes in all recorded interneurones of the appropriate type. The spike frequency during stimulation depended in all cases on the stimulus velocity and originated from the same range of values as the response frequencies of the velocity-sensitive units in the ChO. Inhibitory effects induced by velocity also depended on the magnitude of velocity.

Recent data on interneurones of the midline group in the metathoracic ganglion of the locust (Burrows, 1988) show that several neurones are affected by movement signals from the ChO. In the stick insect no interneurones with comparable properties (morphology, physiology) have been found. Since acceleration-effects of the different stimuli were not investigated in the locust, a detailed comparison of the physiology of the locust interneurones with the physiology of the neurones described here is problematic.

Acceleration elicited exclusively excitatory effects in these interneurones

Thresholds for spike initiation vary over a value range of more than four decades ($0{\cdot}002$–$39{\cdot}7\,m\,s^{-2}$). The smallest thresholds are similar to those of the sensory units ($0{\cdot}002$–$0{\cdot}004\,m\,s^{-2}$) in the ChO (Hofmann & Koch, 1985).

Pure acceleration signals affected the activity of several interneurones. This result points in the direction of the 'alarm hypothesis' of Hofmann & Koch (1985).

Processing of sensory input from different sensory units by single interneurones

Six of the interneurones inhibited by the velocity signals of the ChO stimuli showed excitatory effects in response to acceleration input (Fig. 13; Table 4, nos 6–11). Hofmann & Koch (1985) found velocity and acceleration (V, A) receptors in different combinations in the ChO. None of the sensory units described could induce the effects observed in these interneurones. This means that this type of interneurone (or an interneurone presynaptic to it) has inputs from at least two receptor units of the ChO, one for the velocity signal, the other for the acceleration signal (in Hofmann & Koch's terms V+− and A+−receptors). Thus, it is inferred that the input of functionally different sensory units to the nervous system is processed in single interneurones (see Burrows, 1987).

In addition, interneurones were found to be affected by position, velocity and acceleration (Fig. 3A). Since no units were found in the ChO which measure all three movement parameters (Hofmann *et al.* 1985; Hofmann & Koch, 1985) this finding points in the same direction.

Velocity representation and velocity control

Some interneurones were found to be excited only by positive velocity values (Table 1, row 4). However, in most cases the recorded interneurones were excited by velocities of both signs, i.e. movement in either direction.

About 40 % of the recorded interneurones (23 of 55) were inhibited by velocity input. About 25 % of these (Table 1, rows 6,7) showed velocity-induced inhibition for one sign of velocity only: four neurones reacted only to positive velocities (joint flexion), one interneurone reacted only to negative velocities (joint extension).

In 18 recordings, velocities of both signs elicited inhibition in the interneurone (Table 1, row 5). Just as in the majority of excitatory responses to velocity input, most inhibitory effects do not represent the sign of the velocity at the interneuronal level. Small thresholds of inhibition (in 11 of 15 cases $0{\cdot}3\,mm\,s^{-1}$ or $60\,degrees\,s^{-1}$) also cause the default of information about the absolute value of velocity at the output side of these interneurones.

In summary, velocity is represented in four ways in these interneurones: (a) the sign (direction) and the absolute value of velocity (collected in Table 1, row 4); (b) the absolute velocity value without the sign of the velocity (Table 1, row 3); (c) the sign of the velocity without information about the absolute value (Table 1, rows 6,7); (d) movement indication, without information about the absolute value and the sign of velocity (Table 1, row 5). Interestingly, this was the type most often found.

In stick insects, evidence exists that velocity is controlled in different phases of

walking. Cruse (1985) showed velocity control of the retraction movements in the stance phase; Dean (1984) demonstrated that velocity was controlled during the swing phase of a step. Bässler (1988) has shown that the occurrence of the 'active reaction' to chordotonal organ stimulation is velocity-dependent, but that the transition from flexor to extensor activity (when the active reaction occurs) is independent of the absolute value of velocity. This shows that velocity-sensitive neurones both with absolute-value-dependent and with absolute-value-independent responses are incorporated in the generation of the active reaction.

Even in the standing or inactive animal, velocity might be an important and controlled movement parameter, which is set to zero in this particular situation. Few of the characterized interneurones in this paper had the physiology appropriate for such a controlling task, because they represent the velocity signal incompletely.

Interneurones with excitatory effects on the SETi motoneurone

Some local interneurones with the soma located in the anterior lateral region of the mesothoracic ganglion which were inhibited by velocity signals from the ChO had excitatory effects on the activity of the SETi motoneurone. It is not known if the effects on the SETi are direct or indirect.

Although a connection from the ChO to the SETi motoneurone was shown to be mediated by these interneurones, their physiological characteristics do not indicate that they are involved in the neuronal processes generating the dynamic and static part of the resistance reflex in the SETi motoneurone. Their activities diminish the resistance reflex in the SETi motoneurone.

The totally altered response properties in the active animal prohibit a simple functional interpretation of the physiology of these interneurones. Because such changes of physiological properties were detected in several characterized interneurones (A. Büschges, unpublished results), a definition of the behavioural state of an animal during the experiment becomes necessary.

In the locust, local interneurones have been characterized (Burrows & Watkins, 1986) in the meso- and metathoracic ganglia that have a similar morphological structure. In the locust these interneurones are called the 'anterior-lateral group'. In locusts, it is known that the interneurones of this group get excitatory inputs from external mechanoreceptors on the contralateral leg. The properties of the functional context of this group of interneurones are as yet unknown.

This work was supported by a grant of the Deutsche Forschungsgemeinschaft (Ba 578) to Professor Ulrich Bässler. Professor Fred Delcomyn, Uwe Koch and Rolf Kittmann read this paper in manuscript, and I greatly appreciate their helpful comments. This work would not have been possible without the constant support of Professor U. Bässler.

References

BÄSSLER, U. (1976). Reversal of a reflex to a single motoneurone in the stick insect *Carausius morosus*. *Biol. Cybernetics* **24**, 47–49.

BÄSSLER, U. (1983). *Neural Basis of Elementary Behavior in Stick Insects*. Berlin, Heidelberg, New York: Springer-Verlag.

BÄSSLER, U. (1988). Functional principles of pattern generation for walking movements of stick insect forelegs: the role of the femoral chordotonal organ afferences. *J. exp. Biol.* **136**, 125–147.

BURROWS, M. (1985). The processing of mechanosensory information by spiking local interneurones in the locust. *J. Neurophysiol.* **54**, 463–478.

BURROWS, M. (1987). Parallel processing of proprioceptive signals by spiking local interneurons and motor neurons in the locust. *J. Neurosci.* **7**, 1064–1080.

BURROWS, M. (1988). Responses of spiking local interneurones in the locust to proprioceptive signals from the femoral chordotonal organ. *J. comp. Physiol.* A **164**, 207–217.

BURROWS, M. & WATKINS, B. L. (1986). Spiking local interneurones in the mesothoracic ganglion of the locust: Homologies with metathoracic interneurones. *J. comp. Neurol.* **245**, 29–40.

CRUSE, H. (1985). Which parameters control the leg movement of a walking insect? I. Velocity control during stance phase. *J. exp. Biol.* **116**, 357–362.

DEAN, J. (1984). Control of leg protraction in the stick insect: a targeted movement showing compensation for externally applied forces. *J. comp. Physiol.* A **155**, 771–781.

HOFMANN, T. & KOCH, U. T. (1985). Acceleration receptors in the femoral chordotonal organ of the stick insect, *Cuniculina impigra*. *J. exp. Biol.* **114**, 225–237.

HOFMANN, T., KOCH, U. T. & BÄSSLER, U. (1985). Physiology of the femoral chordotonal organ in the stick insect, *Cuniculina impigra*. *J. exp. Biol.* **114**, 207–223.

LAURENT, G. (1986). Thoracic intersegmental interneurones in the locust with mechanoreceptive inputs from a leg. *J. comp. Physiol.* A **159**, 171–186.

LAURENT, G. (1987*a*). Parallel effects of joint receptors on motor neurones and intersegmental interneurones in the locust. *J. comp. Physiol.* A **160**, 341–353.

LAURENT, G. (1987*b*). The morphology of a population of thoracic intersegmental interneurones in the locust. *J. comp. Neurol.* **256**, 412–429.

LAURENT, G. (1988). Local circuits underlying excitation and inhibition of intersegmental interneurones in the locust. *J. comp. Physiol.* A **162**, 145–157.

SCHMITZ, J. (1986*a*). The depressor trochanteris motoneurones and their role in the coxo-trochanteral feedback loop in the stick insect *Carausius morosus*. *Biol. Cybernetics* **55**, 25–34.

SCHMITZ, J. (1986*b*). Properties of the feedback system controlling the coxa-trochanter joint in the stick insect *Carausius morosus*. *Biol. Cybernetics* **55**, 35–42.

SCHMITZ, J., BÜSCHGES, A. & DELCOMYN, F. (1989). An improved electrode design for *en passant* recording from small nerves. *Comp. Biochem. Physiol.* **91**A, 769–772.

STEWART, W. W. (1978). Functional connections between cells as revealed by dye-coupling with a high fluorescent naphthalimide tracer. *Cell* **14**, 741–759.

WEIDLER, D. J. & DIECKE, F. P. J. (1969). The role of cation conduction in the central nervous system of the herbivorous insect *Carausius morosus*. *Z. vergl. Physiol.* **64**, 372–399.

WEILAND, G., BÄSSLER, U. & BRUNNER, M. (1986). A biological feedback system with electronic input: the artificially closed femur–tibia control system of stick insects. *J. exp. Biol.* **120**, 369–385.